Design and Implementation of a Prototype Sunflower-Type Photovoltaic System

Walter Naranjo Lourido, Luis Alberto Contreras Acosta, Wilver Stivenson Arana Pérez, Javier Eduardo Martínez Baquero

Engineering School, Faculty of Basic Sciences and Engineering, Universidad de Los Llanos, Villavicencio, Colombia (e-mail: wnaranjo@unillanos.edu.co, luis.contreras.acosta@unillanos.edu.co, wilver.arana.perez@unillanos.edu.co, jmartinez@unillanos.edu.co)

Abstract: This paper presents the design of a prototype sunflower-type photovoltaic system with linear PID control for maximizing solar radiation collection. The design process begins with developing a sensing system comprising three key components, transduction of the physical variable into an electrical signal, conditioning the electrical signal for microcontroller Reading, the corresponding processing algorithm. Subsequently, two PID controllers are designed and implemented to position the photovoltaic system at an orthogonal angle relative to solar radiation. Based on the results, it is concluded that the sensing system enables achieving the optimal solar radiation collection angle for the sunflower photovoltaic system. Even with multiple light energy sources, the system searches for the ideal angular positioning to maximize the incidence of light energy. Additionally, the designed PID controller demonstrates a stable response to input changes or external disturbances, enhancing the prototype's accuracy, stability, and speed.

Keywords: Angular positioning, PID control, Prototype sunflower, Solar radiation, Solar tracker.

1. INTRODUCTION

The global rise in energy consumption can be attributed to population growth, economic development, and urbanization, significantly impacting the environment and the global economy (AlAward, 2022, p. 351) (Bazan Navarro et al., 2023). According to data from the International Energy Agency (IEA), global electricity consumption has increased by 25% in the past decade. Coal remains the primary source, accounting for 35% of electricity generation, followed by natural gas at 24%, hydro sources at 17%, and solar systems at 3% (International Energy Agency, n.d.).

Despite the recent surge in electricity consumption, the future of global energy consumption remains uncertain due to various external factors (Y. Zhang et al., 2022). While an increase in consumption is expected due to growing demand in developing countries and the need to meet the energy requirements of a growing population (Mauleón, 2022), it is essential to consider these uncertainties.

Numerous energy consumption challenges have been implemented worldwide to promote sustainability. These strategies include the promotion of renewable energies like wind and solar power (Ağbulut, 2022), improved energy efficiency in industries and households, stricter government policies, and raising public awareness about responsible energy consumption (Fang et al., 2023; J. Zhang et al., 2022). These efforts mitigate energy production and consumption's environmental and economic impacts.

Renewable energies play a significant role in Colombia's energy mix, with hydroelectric, wind and solar power being the main sources (Sagastume Gutiérrez et al., 2020). Over the years, there has been a notable increase in investment and development of renewable energy projects in the country, driven by the objective of reducing dependence on fossil fuels and promoting more sustainable energy solutions (Zapata et al., 2022).

Hydroelectric power stands as the primary source of renewable electricity generation in Colombia. Its wide availability, sustainability, reliability, and ability to meet peak energy demands have contributed to its long-standing implementation (Arias-Gaviria et al., 2019). Simultaneously, wind and solar energy sources are considered emerging sources of energy generation, showing promising potential (Pupo-Roncallo et al., 2019).

Hydroelectric energy accounts for approximately 50% of the country's electricity generation, primarily concentrated in Tolima, Valle del Cauca, Huila, and Quindío. On the other hand, Colombia's coastal regions, such as La Guajira, Magdalena, and Sucre, possess significant wind power generation potential due to their consistent and strong winds (Gil Ruiz et al., 2022).

Colombia benefits from its favorable geographical position, receiving abundant solar radiation year-round. This resource scarcity has spurred the development of solar energy technologies (López et al., 2020).

Solar energy is experiencing remarkable growth as a renewable energy source in Colombia, contributing around 201 GWh to the country's electricity generation. Córdoba, Tolima, and Valle del Cauca are widely recognized as key regions for solar energy production in Colombia (International Energy Agency, s.f).

Unlike wind power systems, which are primarily situated along Colombia's Caribbean and Pacific coasts to maximize efficiency based on wind speed, solar systems can be implemented across various regions in Colombia. This flexibility is due to their consistent power production in the country's coastal and inland areas (Ángel-Sanint et al., 2023).

The conversion of light energy from the Sun into electrical energy is accomplished through the photovoltaic effect. This process involves the interaction of sunlight with a semiconductor material, where photons stimulate electrons, causing them to detach from their original orbits and become free electrons. These electrons then move through the semiconductor material and are captured by the electrodes at the edges, generating electrical energy (Hirst, 2012, pp. 293-313).

Consequently, the amount of electrical energy a solar panel produces depends on the quality of solar radiation it receives at any given moment. Ideally, the solar radiation should be perpendicular to the panel to maximize the conversion of light energy into electricity (Bayod-Rújula, 2019, pp. 237–295).

In recent years, the installation of rooftop solar panels has increased as a sustainable and effective solution for generating renewable energy and reducing carbon footprints in residential and commercial buildings (Ros & Sai, 2023). This installation method involves mounting photovoltaic panels on the building's roof and securing them to a frame or metal rail system. Rooftop solar panels offer the advantage of utilizing available roof space and can be integrated with various roofing materials (Boxwell, 2022).

When installing a solar system, factors such as the angle of incidence, orientation, and geographical location must be considered to optimize electricity generation. The trajectory of the Sun in the sky rises from the east, moves from south to north in the northern hemisphere and from north to south in the southern hemisphere, and sets in the west (Zhong et al., 2022).

Solar systems installed on building roofs typically have a fixed tilt angle for solar panels to maximize power generation. However, large land areas are required to accommodate additional solar panels and meet the energy needs in systems with increasing energy demands. Solar panels are often installed with solar trackers to enhance energy efficiency, which can be adjusted to optimize solar radiation collection throughout the day. The tilt angle of the solar panel refers to its inclination concerning the horizontal plane (Mamodiya & Tiwari, 2021).

While single-axis solar trackers improve system efficiency during the day, their effectiveness throughout the year is limited due to a phenomenon is known as the Analemma, which prevents maximizing efficiency on all days (Hosseini Dehshiri & Firoozabadi, 2023).

The Analemma visually represents the Sun's apparent path as observed from Earth. It demonstrates the Sun's daily divergence in the sky compared to its expected position, caused by the Earth's axial tilt and elliptical orbit instead of a perfect circle. This phenomenon is often depicted as a figure eight shape (Saphiro, 2022, pp. 176-181).

Solar systems are affected by the variation in solar radiation caused by the Analemma. To address this variation, two-axis solar trackers have been developed. These trackers enable the device to rotate in two directions: the tilt angle and the azimuth angle as the rotation angle (Ramful and Sowaruth, 2022, pp. 295-302).

The advantage of using a two-axis solar tracker is its higher efficiency, as it allows the solar panel to be continuously and optimally oriented towards the Sun, resulting in increased solar energy collection throughout the day. Furthermore, continuous Sun tracking minimizes solar panel shading (Hosseini Dehshiri & Firoozabadi, 2023).

This paper aims to describe the procedures involved in creating a prototype solar tracker photovoltaic system with two axes of motion inspired by the behavior and appearance of Helianthus annuus, commonly known as the sunflower.

2. MATERIALS AND METHOD

The methodology described in Fig. 1 was followed for the project's development

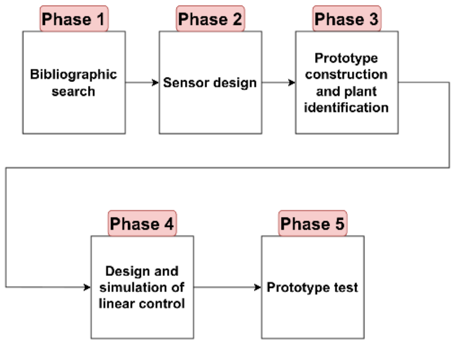

Figure 1. Methodology by phases.

Phase 1 entails conducting extensive research, reviewing, and analyzing pertinent information to lay the groundwork for the project.

Phase 2 involves designing and constructing a sensing system that can accurately determine the position of the sun in the sky.

Phase 3 focuses on physically constructing the prototype to study the sensor's behavior and the plant without any control, aiming to establish its mathematical model.

Phase 4 entails designing and simulating the system to predict its behavior and evaluate its efficiency.

Phase 5 involves testing the prototype with linear control to assess its performance in comparison to the simulated behavior.

2.1 Sensor Transducer

A light radiation transducer from the sun was essential to enable the system to accurately detect the sun's position in the sky and optimize energy capture by the photocells throughout the day. This sun-tracking process aimed to enhance the efficiency of the photovoltaic system, as depicted in Fig. 2.

Various commonly used devices are available within the transducer market, such as Light Dependent Resistors (LDR), photocells, photodiodes, and phototransistors. For this project, photoresistors were chosen for their simplicity and affordability, making them suitable for measuring ambient light in low-budget applications.

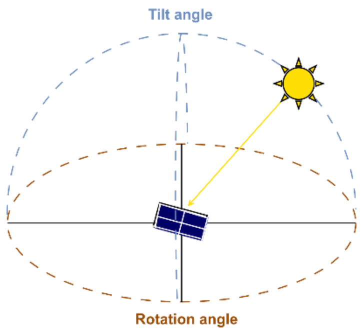

Figure 2. Axes of the solar dome.

It is worth noting that photoresistors are passive devices that exhibit variable electrical resistance in response to the intensity of light they are exposed to. However, it is important to acknowledge that photoresistors have certain limitations. Compared to similar devices like photodiodes or phototransistors, photoresistors generally have lower sensitivity and slower response speeds (Bauman, 2023, Chapter Optical Sensors).

Once photoresistors were chosen as the sensing system's transducers, ensuring their arrangement's accuracy and precision became a top priority. Therefore, the selection and arrangement of photoresistors are crucial to guarantee the reliability and optimal performance of the electrical sensing system.

The characterization process to identify the photoresistors with the least deviation was conducted on 20 units. Various light stimuli were applied to these photoresistors, and their corresponding changes were recorded for analysis, as depicted in Fig. 3 and Fig. 4.

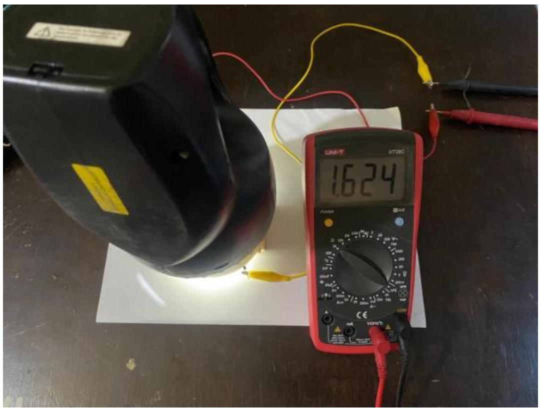

Figure 3. The electrical resistance of an LDR under the influence of a light stimulus.

Figure 4. LDR under the influence of a filtered light stimulus

Table 1 shows the results of the five photoresistors with the least deviation in their electrical resistance to different light stimulation.

Table 1. Characterization of the implemented LDR´s

LED	Unfiltered light (KΩ)	Red filter light (KΩ)	Green filter light (KΩ)	Blue filter light (KΩ)	Deviation (%)
1	2,5	3,4	2,7	2,7	7,91%
4	2,4	3,4	2,6	2,8	7,50%
5	3,0	3,3	2,8	2,4	6,12%
9	3,0	3,3	2,6	2,9	6,61%
10	2,4	3,3	2,7	2,7	3,70%

2.2 Sensor Design

Four LDRs were strategically placed at the sensor's base, which has an octagonal prism shape, to ensure precise positioning and capture of solar radiation. Each LDR was positioned at a 90-degree angle to a plane, simulating the cardinal points of a compass. A tilt of -15 degrees was also introduced to enable radiation capture in a three-dimensional plane. A fifth LDR, placed at the center of the base without inclination, was responsible for capturing radiation orthogonally.The LDRs were connected to the microcontroller through a photoresistor array, a common configuration in light detection applications. In this array, each LDR was positioned at a specific location and connected in series by columns. Each LDR was also connected to a diode for protection and individual readout purposes.

A 5-volt voltage source was connected to each column of photoresistors to measure the voltage across each resistor. It is worth noting that as solar radiation on an LDR increases, the resistor voltage also increases, allowing for the detection and measurement of solar radiation levels.

The signal processing of the photoresistors involved two crisscrossed lines in a cross formation. One line was responsible for determining the tilt angle, while the other line determined the azimuth angle. The photoresist line was initially analyzed to calculate the angles, as illustrated in Fig. 5. The resistors were positioned at angles of 135°, 90°, and 45° on a polar plane. Vectors with magnitudes equal to the input voltage of the microcontroller were projected at these angles. A vector sum of these three vectors was then performed to determine the vector indicating the angle of the highest solar radiation.

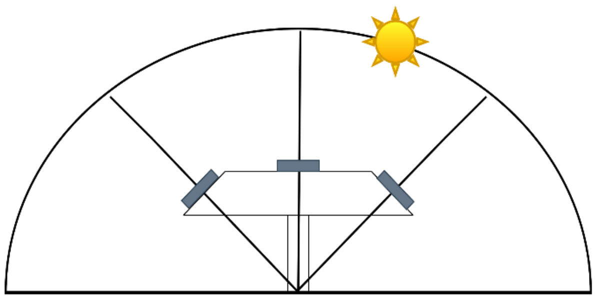

Figure 5. LDR line diagram.

Using separate lines for the tilt and azimuth angles enhances the precision of measuring the sun's direction. The system effectively determines the angle representing the highest solar radiation by employing the vector summation technique with the vectors projected at specific angles. This signal-processing approach ensures the measurement of the sun's direction is accurate and dependable, contributing to the overall reliability of the photoresistor-based system.

2.3 3D modeling of the prototype

Once the sensing system responsible for locating the sun's position in the solar dome was designed, the prototype was physically built to capture data on its behavior. In this process, 3D printing technology was used to manufacture the required parts.

1) Sensor support: The sensor base was designed in the shape of an octagonal prism to secure the LDRs of the sensor on four of the eight opposite sides and to obtain four LDRs arranged at 90 degrees to each other. A fifth LDR was placed at the midpoint of the LDRs to serve as an ideal radiation reference. In addition, the base was tilted to an inclination of -15 degrees to capture the radiation in a three-dimensional plane. In Fig. 6, the 3D modeling of the support is shown

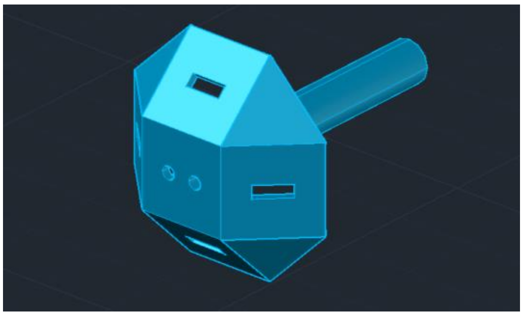

Figure 6. AutoCad sensor support.

2) Actuator support: The installation has three actuators, two of which track solar radiation through movements in the tilt and azimuth angles. The third actuator is responsible for controlling the movement of the solar panels. The supports must allow the three actuators to move simultaneously. In Fig. 7, the 3D modeling of the bracket is shown.

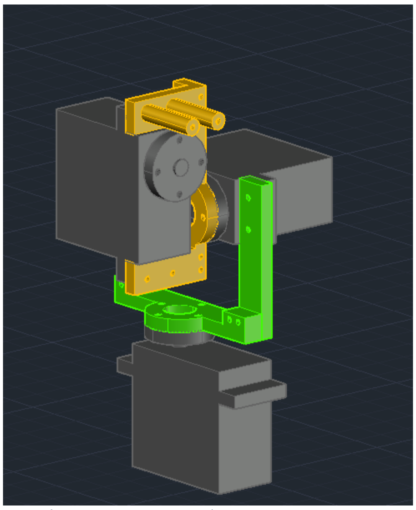

Figure 7. AutoCad actuator support.

3) Panel support: Sunflower systems are characterized by the arrangement of the solar panels in a pattern that mimics the petals of a sunflower. In addition, the support used in this system must be able to close the petals to protect them from weather phenomena. The 3D modeling of the support is shown in Fig. 8.

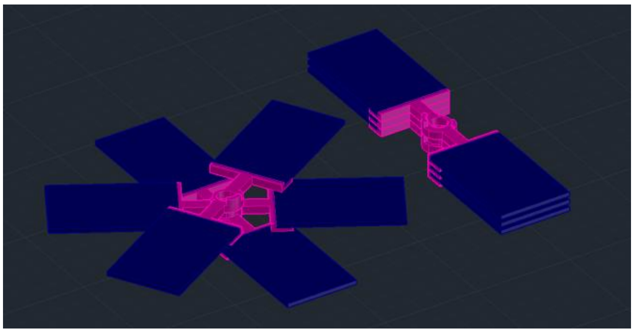

Figure 8. AutoCad solar panels support.

With the parts modeled in AutoCAD for the sensing system, actuators, and solar panels, a model of the assembled parts was made to corroborate their design, as shown in Fig. 9.

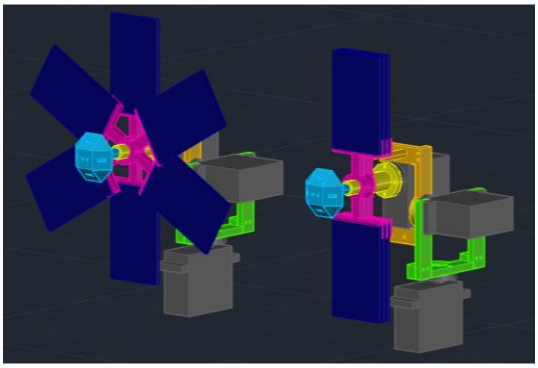

Figure 9. 3D modeling of the prototype sunflower-type photovoltaic system.

A. *Proportional-integral-derivative controller (PID)*

The system utilizes servomotors as actuators, which have a mechanical limitation of movement of 180°. These servomotors consist of a DC motor, a gear set, and a potentiometer serving as an angular position sensor. They operate discretely with predefined frequencies, and modern microcontrollers offer libraries to convert desired angles into motor frequencies. However, relying on these libraries restricts the working resolution to one degree. For greater precision, the control signal will be manipulated across the operating frequency range of the servo motor.

Designing the linear control for the servomotors necessitates obtaining the mathematical model of the system. Two methodologies exist for acquiring the transfer function of a system. The first method involves determining the function from the parameters of the system components, which requires detailed knowledge of the plant to derive the transfer function. The second method is system identification, which involves analyzing the input and output signals of the system to develop a mathematical model that accurately represents the plant's behavior.

A step-type input was applied to identify each servomotor, inducing magnitude changes at specific time intervals to record the motor's behavior and determine a suitable mathematical model that aligns with the observed characteristics, as depicted in Fig. 10 and Fig. 11.

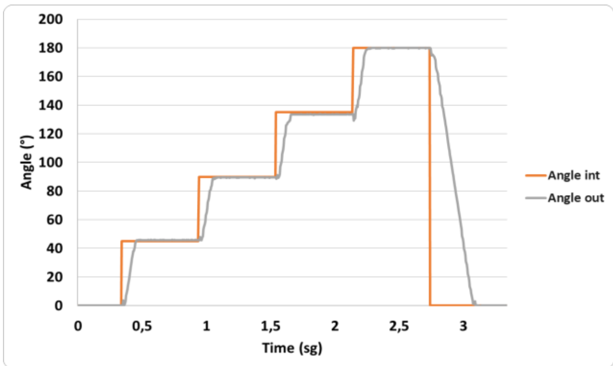

Figure 10. Behavior of the servomotor in charge of the tilt angle displacement.

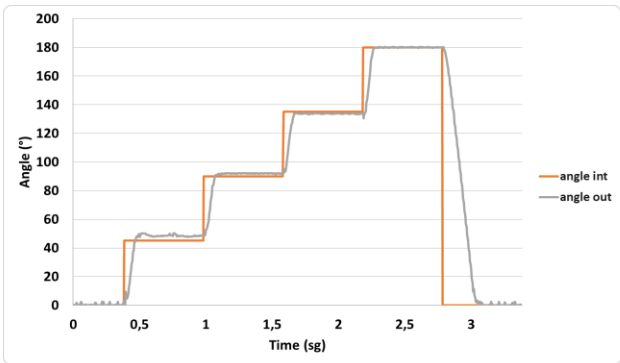

Figure 11. Behavior of the servomotor in charge of the azimuth angle displacement.

As a result, the following transfer functions were obtained for each of the motors:

$$TF = \frac{213.3s + 47.72}{s^3 + 27.12s^2 + 215.3s + 51.41} \quad (1)$$

$$TF = \frac{163.8s + 388.3}{s^3 + 33.53s^2 + 212.3s + 381.5} \quad (2)$$

The mathematical models for both the servomotor (1) controlling the azimuth angle displacement and (2) the servomotor controlling the tilt angle displacement have been established.

After obtaining the mathematical model of the system, it is crucial to assess its inherent stability. The controller's configuration, such as the PID controller, can enhance or diminish the system's stability. However, if the system is already unstable, implementing a PID controller may worsen the situation instead of improving it. Analyzing the stability of the uncontrolled system provides a deeper understanding of its behavior and helps determine the most suitable controller for the application.

Various techniques exist to determine the inherent stability of a system without a controller, such as step response analysis or Jacobian matrix analysis. In this work, the root locus stability criterion was employed. This technique involves plotting the geometric locus of the roots of the system's characteristic polynomial in the complex plane. By analyzing the root locus, it becomes possible to determine whether the system's poles are in the left half-plane of the complex plane (indicating stability), on the imaginary axis (indicating marginal stability), or in the right half-plane (indicating instability).

Fig. 12 illustrates the location of the roots of the transfer functions (1) and (2). It can be observed that the poles of the servomotor responsible for the azimuth angle movement are situated in the left half-plane, indicating the stability of this actuator. Similarly, the poles of the servomotor responsible for the tilt angle movement are also located in the left half-plane, confirming the stability of the tilt actuator. Additionally, it can be analyzed that the poles of the tilt servomotor are closer to the imaginary axis than the other servomotor, and their imaginary component is smaller. Consequently, these poles suggest that the servomotor controlling the tilt angle displacement will exhibit faster dynamics and a more stable behavior than the other servomotor.

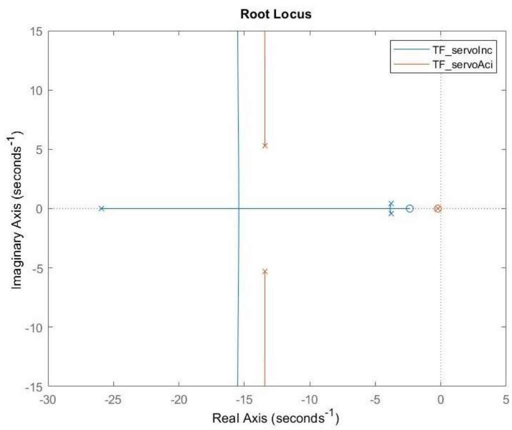

Figure 12. Location of actuator roots.

After confirming the stability of the transfer functions, the next step was to design a linear controller. Since the controller operates through a microcontroller, converting the system from continuous to discrete time was necessary. This conversion unit for each transfer function was employed to meet the bandwidth criterion and settling time. This process allowed us to determine the appropriate sampling time interval for the conversion to discrete time. The zero-order hold method, widely used in digital control, converted the transfer functions from continuous to discrete time. Sisotool was used to adjust the PID parameters for each motor. Several parameters were established, including a maximum overshoot of less than 2% and a settling time of 2 seconds. By applying these criteria, the following equations were derived:

$$0.224 + 2.24\frac{Ts}{z-1} + 0.005\frac{z-1}{Ts} \quad (3)$$

$$0.459 + 2.12\frac{Ts}{z-1} + 0.024\frac{z-1}{Ts} \quad (4)$$

Being (3) the parameters of the PID controller of the servomotor in charge of the azimuth angle displacement and (4) the parameters of the PID controller of the servomotor in charge of the tilt angle displacement, we have that the Ts value for both equations is 0.1.

3. RESULTS AND DISCUSSIONS

3.1. Simulations

With the PID controller designed, we performed the corresponding simulations in each actuator using the Simulink software of Matlab. The simulations for each servomotor are divided into two sections; the first section is simulated with Simulink Step and Ramp functions to model the behavior of the LDR corresponding to a light stimulus; the simulated LDR magnitude enters a function block that performs an algorithm similar to the microcontroller to calculate the angle orthogonal to the ideal solar incidence angle. The second section takes the reference angle to a closed-loop system with the PID controller and the plant transfer function to analyze its behavior compared to the open-loop plant transfer function. Fig. 13 shows the block programming in Simulink for the servomotor in charge of the inclination.

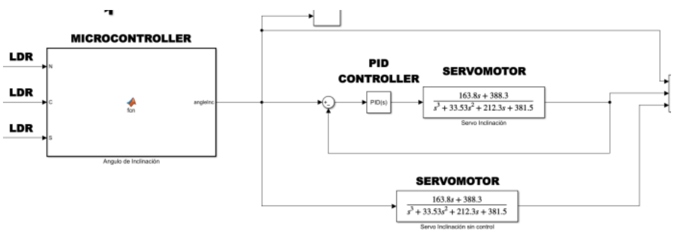

Figure 13. Simulation in Matlab's Simulink.

Fig. 14 shows the input signal of the LDRs as a step input and its output at the angle calculated by the microcontroller to maximize radiation collection in the solar panels.

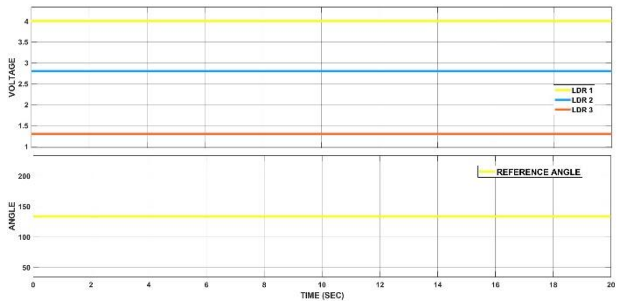

Figure 14. Conversion from step input to a reference angle.

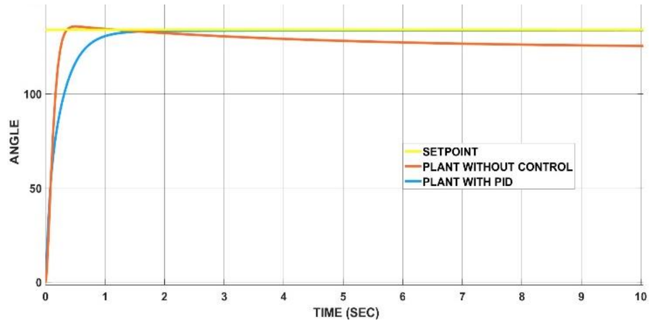

Figure 15. Controller and plant output with step type input.

Fig. 15 shows the reference signals drawn in yellow color, the output of the plant without control drawn in orange color, and the output of the plant with linear control drawn in blue color. It can be observed that the controlled signal has a reduction of the stationary error and does not present maximum overshoot; however, its rise time is higher by a small margin.

In Fig. 16, the input signal of the LDRs as input has a ramp-type behavior and its output at the angle calculated by the microcontroller to maximize the collection of radiation in the solar panels at the instant of time.

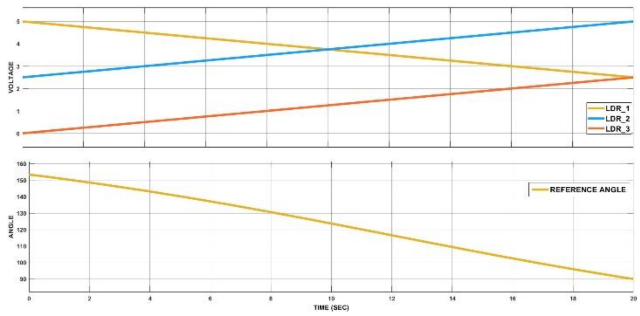

Figure 16. Conversion of ramp type input to a reference angle.

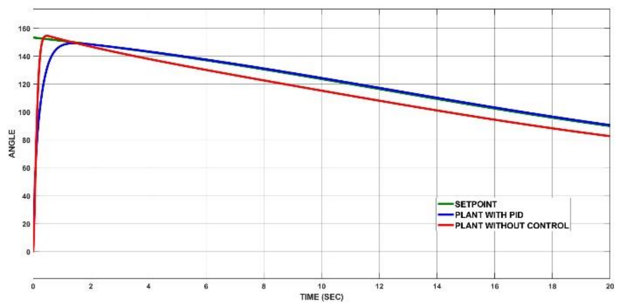

Figure 17. Controller and plant output with ramp type input.

Fig. 17 shows the reference signals drawn in green, the plant without control drawn in red, and the plant's output with linear control drawn in blue. It can be observed that the controlled signal has a reduction of the stationary error and does not present maximum overshoot; however, its rise time is longer.
When comparing the behaviors of the plant simulations, it is observed that the uncontrolled steady state error tends to zero for the step-type inputs and is constant for the ramp-type inputs. Therefore, the actuators are type 1 systems.
After analyzing the results obtained from the simulations of the linear PID controller designed for each actuator, it can be concluded that the controller's performance is satisfactory. Furthermore, it is important to highlight that using simulation techniques allowed a rigorous and detailed evaluation of the controller behavior in different scenarios, which provides greater confidence in its performance in the physical prototype.

3.2. Scale prototype

The scaled prototype of the sunflower-type photovoltaic system is built regarding the 3D modeling done, as shown in Fig. 18. The prototype meets the specifications designed in the 3D modeling to comply with the proposed behavior.

Figure 18. Sunflower scale prototype.

During the construction process, a limitation arose because the cable connections of the elements did not allow endless rotation of the servomotor in charge of the azimuth angle. Therefore, to avoid cable winding in the prototype, the rotation of the servomotor was limited from -180° to 180°, which allowed 360° of rotation coverage and avoided cable winding at the zero-angle crossing.
To analyze the behavior of the prototype with the developed method for solar radiation tracking and the designed PID controller was decided to implement a control methodology based on logic operations with the magnitude of the LDRs; Fig. 19 shows the flow diagram of this methodology.

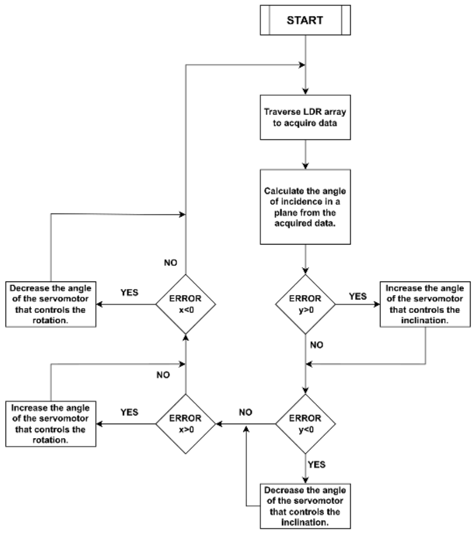

Fig 19. Logic operation control diagram.

With the implementation of the controller by logical operations in the prototype, it could be observed that its behavior is accurate but with a high settling time. This settling time is because the servomotors are displaced a certain number of degrees in the plane before performing a new error calculation. Therefore, the smaller the displacement, the more iterations are required to reach the ideal angle, although minimal error will be obtained in the system.
By implementing the PID controller in the prototype sunflower-type PV system, tracking the light radiation source with the largest incident magnitude is observed to be precise and accurate. In addition, the response speed of the prototype is improved due to the implementation of the PID controller. Fig. 20 shows the prototype tracking a light energy source.

Figure 20. Scale prototype following light from a flashlight.

4. CONCLUSIONS

Designing a sensing system for localizing the solar radiation source as possible, which works successfully. Guarantee the system's reproducibility and repeatability is important to

consider the variability in the behavior of the same model's transducers and select those with less standard deviation between them.
During the design process of the linear PID controller for the spatial positioning of the actuators, its transfer functions were used as a basis, considering the system's stability by analyzing its root locus. Furthermore, before implementing the controller in the scale prototype, simulations of the system with various inputs were carried out to ensure its correct operation.
During the construction of the scaled prototype of the sunflower PV system, 3D modeling and printing were used to ensure the stability of the structure. Once commissioned, it was possible to observe the precise movement of the solar panels to capture maximum light radiation, even when multiple sources of incident light energy were presented to the prototype.

REFERENCES

Ağbulut, Ü. (2022). A novel stochastic model for very short-term wind speed forecasting in the determination of wind energy potential of a region: A case study from Turkey. Sustainable Energy Technologies and Assessments, 51(101853), 101853. https://doi.org/10.1016/j.seta.2021.10185.

AlAwad, M. N. J. (2022). Remarks on the world's current energy supply and demand. Journal of King Saud University - Engineering Sciences, 34(7), 351. https://doi.org/10.1016/j.jksues.2022.09.001

Ángel-Sanint, E., García-Orrego, S., & Ortega, S. (2023). Refining wind and solar potential maps through spatial multicriteria assessment. Case study: Colombia. Energy for Sustainable Development: The Journal of the International Energy Initiative, 73, 152–164. https://doi.org/10.1016/j.esd.2023.01.019

Arias-Gaviria, J., Carvajal-Quintero, S. X., & Arango-Aramburo, S. (2019). Understanding dynamics and policy for renewable energy diffusion in Colombia. Renewable Energy, 139, 1111–1119. https://doi.org/10.1016/j.renene.2019.02.138

Baumann, P. (2023). Optical Sensors. In Selected Sensor Circuits (pp. 43–101). Springer Fachmedien Wiesbaden.

Bavafa-Toosi, Y. (2017). Root locus. In Introduction to Linear Control Systems (pp. 351–441). Elsevier.

Bayod-Rújula, A. A. (2019). Solar photovoltaics (PV). In Solar Hydrogen Production (pp. 237–295). Elsevier.

Bazán Navarro, C. E., Álvarez-Quiroz, V. J., Sampi, J., & Arana Sánchez, A. A. (2023). Does economic growth promote electric power consumption? Implications for electricity conservation, expansive, and security policies. Electricity Journal, 36(1), 107235. https://doi.org/10.1016/j.tej.2023.107235

Boxwell, M. (2022). Solar Electricity Handbook - 2022 Edition: A simple, practical guide to solar energy: how to design and install photovoltaic solar electric systems. Greenstream Publishing.

El Hammoumi, A., Chtita, S., Motahhir, S., & El Ghzizal, A. (2022). Solar PV energy: From material to use, and the most commonly used techniques to maximize the power output of PV systems: A focus on solar trackers and floating solar panels. Energy Reports, 8, 11992–12010. https://doi.org/10.1016/j.egyr.2022.09.054

Fang, G., Chen, G., Yang, K., Yin, W., & Tian, L. (2023). Can green tax policy promote China's energy transformation? A nonlinear analysis from production and consumption perspectives. Energy (Oxford, England), 269(126818), 126818. https://doi.org/10.1016/j.energy.2023.126818

Gil Ruiz, S. A., Cañón Barriga, J. E., & Martínez, J. A. (2022). Assessment and validation of wind power potential at convection-permitting resolution for the Caribbean region of Colombia. Energy (Oxford, England), 244(123127), 123127. https://doi.org/10.1016/j.energy.2022.123127

Haidekker, M. A. (2020). Stability analysis for linear systems. In Linear Feedback Controls (pp. 145–156). Elsevier.

Hirst, L. C. (2012). Principles of solar energy conversion. In Comprehensive Renewable Energy (pp. 293–313). Elsevier.

Hosseini Dehshiri, S. S., & Firoozabadi, B. (2023). Comparison, evaluation and prioritization of solar photovoltaic tracking systems using multi criteria decision making methods. Sustainable Energy Technologies and Assessments, 55(102989), 102989. https://doi.org/10.1016/j.seta.2022.102989

International Energy Agency. (n.d.). Energy Statistics Data Browser. IEA. Retrieved January 15, 2023, from https://www.iea.org/data-and-statistics/data-tools/energy-statistics-data-browser?country=COLOMBIA&fuel=Energy%20supply&indicator=TESbySource

López, A. R., Krumm, A., Schattenhofer, L., Burandt, T., Montoya, F. C., Oberländer, N., & Oei, P.-Y. (2020). Solar PV generation in Colombia - A qualitative and quantitative approach to analyze the potential of solar energy market. Renewable Energy, 148, 1266–1279. https://doi.org/10.1016/j.renene.2019.10.066

Mamodiya, U., & Tiwari, N. (2021). Design and implementation of an intelligent single axis automatic solar tracking system. Materials Today: Proceedings. https://doi.org/10.1016/j.matpr.2021.04.428

Mauleón, I. (2022). A statistical model to forecast and simulate energy demand in the long-run. Smart Energy, 7(100084), 100084. https://doi.org/10.1016/j.segy.2022.100084

Pupo-Roncallo, O., Campillo, J., Ingham, D., Hughes, K., & Pourkashanian, M. (2019). Large scale integration of renewable energy sources (RES) in the future Colombian energy system. Energy (Oxford, England), 186(115805), 115805. https://doi.org/10.1016/j.energy.2019.07.135

Ramful, R., & Sowaruth, N. (2022). Low-cost solar tracker to maximize the capture of solar energy in tropical countries. Energy Reports, 8, 295–302. https://doi.org/10.1016/j.egyr.2022.10.145

Ros, A. J., & Sai, S. S. (2023). Residential rooftop solar demand in the U.S. and the impact of net energy metering and electricity prices. Energy Economics, 118(106491), 106491. https://doi.org/10.1016/j.eneco.2022.106491

Sagastume Gutiérrez, A., Balbis Morejón, M., Cabello Eras, J. J., Cabello Ulloa, M., Rey Martínez, F. J., & Rueda-Bayona, J. G. (2020). Data supporting the forecast of electricity generation capacity from non-conventional renewable energy sources in Colombia. Data in Brief, 28(104949), 104949. https://doi.org/10.1016/j.dib.2019.104949

Shapiro, F. R. (2022). The position of the sun based on a simplified model. Renewable Energy, 184, 176–181. https://doi.org/10.1016/j.renene.2021.11.084

Zapata, S., Castaneda, M., Aristizabal, A. J., & Dyner, I. (2022). Renewables for supporting supply adequacy in Colombia. Energy (Oxford, England), 239(122157), 122157. https://doi.org/10.1016/j.energy.2021.122157

Zhang, J., Abbasi, K. R., Hussain, K., Akram, S., Alvarado, R., & Almulhim, A. I. (2022). Another perspective towards energy consumption factors in Pakistan: Fresh policy insights from novel methodological framework. Energy (Oxford, England), 249(123758), 123758. https://doi.org/10.1016/j.energy.2022.123758

Zhang, Y., Zhang, Y., Zhang, Y., & Zhang, C. (2022). Effect of physical, environmental, and social factors on prediction of building energy consumption for public buildings based on real-world big data. Energy (Oxford, England), 261(125286), 125286. https://doi.org/10.1016/j.energy.2022.125286

Zhong, Q., Nelson, J. R., Tong, D., & Grubesic, T. H. (2022). A spatial optimization approach to increase the accuracy of rooftop solar energy assessments. Applied Energy, 316(119128), 119128. https://doi.org/10.1016/j.apenergy.2022.119128